Gianotti, E.; Díaz Morales, UM.; Coluccia, S.; Corma Canós, A. (2011). Hybrid organic-inorganic catalytic mesoporous materials with proton sponges as building blocks. Physical Chemistry Chemical Physics. 13(24):11702-11709. doi:10.1039/c1cp20588a.

Organic-inorganic mesoporous materials with walls built of proton sponges for base catalysis

E. Gianotti[a,b], *U. Diaz*[a], *S. Coluccia*[b], *A. Corma*[a*]

[a]Instituto de Tecnología Química (UPV-CSIC) Universidad Politécnica de Valencia. Consejo Superior de Investigaciones Científicas. Avenida de los Naranjos s/n., 46022 Valencia. Spain.

[b]Department of Chemistry IFM and NIS-Centre of Excellence, University of Turin V. P. Giuria 7 – 10125 Turin (Italy).

Abstract

Non ordered organic-inorganic mesoporous hybrid materials with basic sites have been synthesized following a fluoride-catalysed sol-gel process, at neutral pH and low temperatures that avoids the use of structural directing agents (SDAs). Proton sponges have been used as the organic builder of the hybrids, while the inorganic part corresponds to silica tetrahedra. The proton sponges are diamines that exhibit very high basicity and, after functionalization, have been introduced as part of the walls of the mesoporous silica by one-pot synthesis. Several hybrids with different organic loadings have been synthesized and characterized by gas adsorption, thermogravimetric and elemental analysis, solid state MAS-NMR and FTIR spectroscopy. These hybrids show high activity as base catalysts and can be recycled

Introduction

The organic-inorganic hybrid porous materials have attracted great attention in the last decade due to their improved or unusual properties that open promising applications in different areas such as optics, electronics, energy, environment, biology, medicine and catalysis.[1,2] In the field of heterogeneous catalysis, the organic-inorganic hybrids offer the advantage to merge the properties of inorganic materials (high mechanical, thermal and structural stability) and of organic moieties (flexibility and functionality).[3] Since the type of the active sites that can be introduced in the inorganic catalysts is limited, whilst the organic molecules can be functionalized to catalyse a larger variety of reactions but suffer from their inability to be recycled, the production of new organic-inorganic hybrids may overcome these drawbacks. In fact, in the hybrid materials, specific catalytic functions are introduced by the structural insertion of the organic moieties, while the inorganic part allows heterogenizing the catalyst and increases the stability; in this way, multifunctional materials should be obtain.[4] Different routes can be followed to synthesise organic-inorganic hybrid catalysts that include: adsorption of the organic species inside the pores of the inorganic host, inclusion of the organic within the pores of the support by “ship in a bottle” type procedure, grafting the desired

organic moiety to the functional groups of the inorganic support, and one-pot synthesis of a composite material with the organic located into the walls of the pores.[1,4,5]

In the last approach, the use of bridged silsesquioxanes ($(R'O)_3SiRSi(OR')_3$) as precursors is decisive to incorporate organic builders into the framework of periodic mesoporous organosilicas (PMOs) following self-assembling routes.[1,6] The presence of different active sites (acid, basic or redox) in the organic linkers contained in the silsesquioxane monomers generates specific multifunctional catalytic materials. For this purpose, surfactants or organic molecules, that are not always easily accessible, are used as structural directing agents (SDAs) to obtain ordered mesoporous hybrids. The possibility to avoid the use of SDAs could be of interest if the hybrids obtained present a high surface area within a narrow and controlled pore size distribution. In this sense, sol-gel processes can be used to synthesise materials due to the low temperature processing, high homogeneity of the solid synthesized and their ability to produce ordered and non-ordered porous materials with controlled textural properties.[7-10] In particular, sol-gel methods based on a fluoride-catalysed route can be of interest when compared with the conventional basic or acid routes, since the former method allows performing the synthesis at nearly neutral pH and room temperature.[11-13] The fluoride-catalysed route is simple and low cost and has been successfully used as a "one-pot" method to synthesise organic-inorganic non-ordered porous materials when functionalized silanes are used during the synthesis process.[13]

In this work, organic-inorganic hybrid materials with a proton sponge as the organic builder have been synthesized following a fluoride-catalysed sol-gel process, at neutral pH and low temperatures, that avoids the use of SDAs.[13,14] The proton sponges are diamines with neighboring atoms at short distance and aromatic frames, such as naphthalene and phenanthrene.[15] These molecules exhibit high unusual basicity, being 1,8-bis(dimethylamino)naphthalene (DMAN, scheme 1) with pK_a=12.1, the archetype of proton sponge.

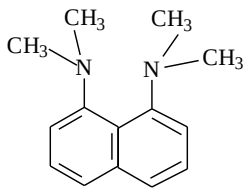

Scheme 1 - scheme of 1,8-bis(dimethylamino)naphthalene (DMAN).

It is accepted that the high basicity constants of the proton sponges are due to steric strains. In DMAN, for example, is not possible to bring even one of the dimethylamino groups into the plane of the rings, resulting in a very low resonance interaction between the nitrogen lone pairs and the

aromatic rings.[16-18] The extreme steric hindrance of DMAN and the destabilizing effect of the overlap of nitrogen lone pairs of the neutral diamines explain the formation of strong N-H-N hydrogen bonds upon monoprotonation, leading to a considerable relaxation of the steric strain. This strong basic molecule has been used as an effective organo-catalyst[19,20] and as an heterogeneous catalyst, after a post-synthesis grafting of the DMAN on a MCM-41,[21] for Knoevenagel condensation reactions. However, some problems with the mesoporous hybrid materials obtained by anchoring of organic moieties were observed, such as the inhomogeneous distribution of active functions into the channels or the partial blockage of the free path within the pores. To overcome these drawbacks, DMAN has been modified here and two terminal reactive silyl groups able to perform co-condensation with a conventional organosilane (TMOS) through sol-gel routes have been introduced. This method has allowed to directly introduce the functionalized DMAN builders into the walls of mesoporous silica by one-pot synthesis. The synthesized hybrids were studied as base catalysts for Knoevenagel condensation of benzaldehyde with active compounds containing activated methylenic groups. Their reactivity has been compared with the homogeneous catalyst and several catalyst recycles were performed to evaluate catalyst deactivation and reusability.

2. Experimental methods

2.1 Synthesis

2.1.1 Preparation of disilylated-proton sponge (DMAN-Si)

The 1,8-bis(dimethylamino)naphthalene (DMAN) was functionalized by the insertion of nitro groups in the naphthalene molecule using a mixture of HNO_3 and H_2SO_4. The reaction mixture was neutralized with aqueous ammonium hydroxide. The nitro groups were reduced to the amino in H_2 using Pd/C as catalyst and, finally, the amino-DMAN was silylated using 3-(triethoxysilyl)propylisocyanate to obtain DMAN-Si. All the steps of DMAN functionalisation (Scheme 2) were followed by liquid (^1H, ^{13}C, ^{29}Si) NMR (see Fig. S1 and S2). In particular, the ^1H NMR spectrum of the silylated DMAN shows a signal at 6.11 ppm assigned to NH groups attached to aromatic rings.[21]

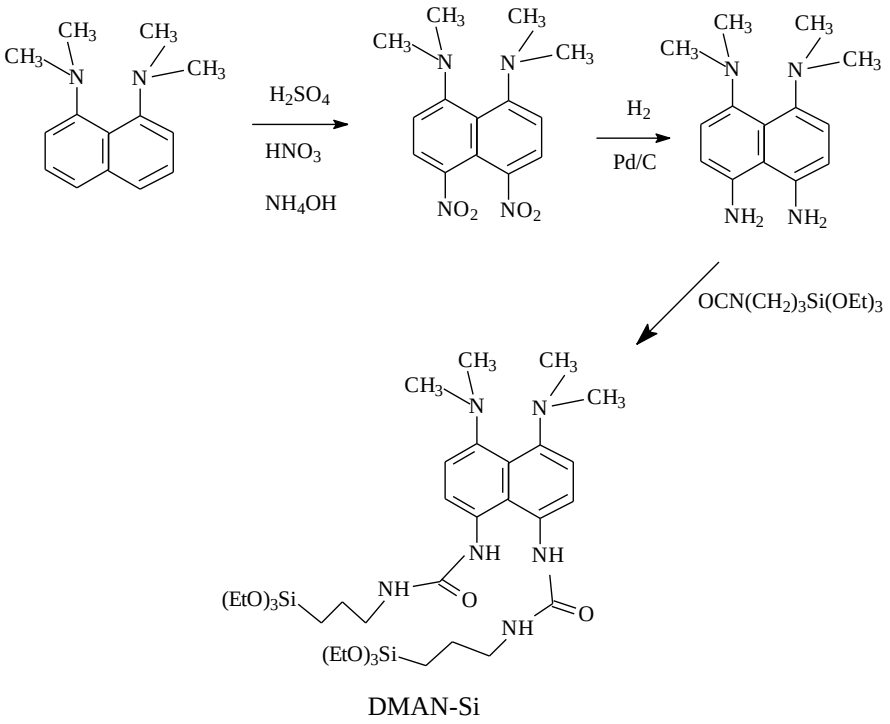

Scheme 2- Scheme of the DMAN functionalisation

2.1.2 Synthesis of the hybrid materials

DMAN/SiO_2 hybrids were synthesized using a NH_4F co-condensation route. Tetramethyl orthosilicate (TMOS) and disilylated-DMAN (DMAN-Si) were mixed in methanol at 298K. After dissolution of precursors, a water solution of NH_4F was added under vigorous stirring.

The final reaction mixture has the following molar composition:

1-x SiO_2: x DMAN-Si: 4 MeOH : 4 H_2O : 0.00313 NH_4F

Hydrolysis and condensation of the silicon precursor was carried out under vigorous stirring at 298K until gelation occurred. Then, the gel was aged at 36°C for 24h and finally dried at 60°C for 24 h. Several hybrids with different DMAN loadings, from x=0.001 to x= 0.1, were synthesized (Table 1). Additionally, DMAN, without terminal silyl groups, was physically adsorbed during the NH_4F co-condensation route of the silica, and pure SiO_2 was also produced following the NH_4F sol-gel route.

Leaching tests were performed by washing the hybrids for 3 days in ethanol at 298K.

In Table 1, the acronyms for the synthesized hybrids and the loading of DMAN are reported.

Table 1. Acronyms of the hybrid materials and DMAN loadings.

Sample Acronyms	DMAN loading **x**	
DMAN/SiO_2-0.1	0.001	
DMAN/SiO_2-0.2	0.002	DMAN-Si in SiO_2 framework
DMAN/SiO_2-0.5	0.005	
DMAN/SiO_2-1	0.01	
DMAN/SiO_2-5	0.05	
DMAN/SiO_2-10	0.10	
ADS-DMAN/SiO_2	0.05	Physically adsorbed DMAN
SiO_2	-	Pure silica

2.2 Characterization of the hybrids

All the hybrids were characterized by N_2 adsorption, thermogravimetric and elemental analyses, solid state MAS-NMR (^{13}C, ^{29}Si) and FTIR spectroscopy.

C, N and H contents were determined with a Carlo Erba 1106 elemental analyzer. Thermogravimetric and differential thermal analyses (TGA-DTA) were recorded in nitrogen stream with a Metler Toledo TGA/SDTA 851E instrument. Volumetric analyses were performed by nitrogen adsorption isotherms at 77K with a Micromeritics ASAP2010. Before the measurements, the samples were outgassed for 12 hours at 100°C. The BET specific surface area[22] was calculated from the nitrogen adsorption data in a relative pressure range from 0.04 to 0.2. The total pore volume[23] was obtained from the amount of N_2 adsorbed at a relative pressure of ~ 0.99. External surface area and micropore volume were estimated with the t-plot method in the t range from 3.5 to 5. The pore diameter and the pore size distribution were obtained following the Barret–Joyner–Halenda (BJH) method[24] on the adsorption branch of the isotherms.

Solid state MAS-NMR spectra were recorded at room temperature under magic angle spinning (MAS) in a Bruker AV-400 spectrometer. The single pulse ^{29}Si spectra were acquired at 79.5 MHz with a 7 mm Bruker BL-7 probe using pulses of 3.5 μs corresponding to a flip angle of 3/4 p radians, and a recycle delay of 240 s. For the ^{13}C cross-polarization (CP) spectra. A 7 mm Bruker BL-7 probe was used at a sample spinning rate of 5 kHz. ^{13}C and ^{29}Si were referred to adamantane and tetramethylsilane, respectively.

FTIR spectra were obtained with a Nicolet 710 spectrometer (4 cm^{-1} resolution) using a conventional greaseless cell. Wafers of ca.10 mg cm^{-2} were outgassed at room temperature, 100ºC, 200ºC and 400ºC overnight.

Thermogravimetric analysis, solid state MAS-NMR and FTIR characterization have only been performed with the high loading hybrids, since with the low loading samples, the intensity of the signals due to the organic moiety was too weak.

2.3 Catalytic tests

The hybrid catalysts were tested for the Knoevenagel condensation. The catalysts used were previously washed for 3 days in ethanol to remove the un-reacted DMAN-Si molecules. Before catalytic tests, all the catalysts were outgassed at 373K for 12h to remove physisorbed water. A mixture of benzaldehyde (8 mmol) and ethyl cyanoacetate (7 mmol) was stirred at the desired reaction temperature (333K) using ethanol as solvent under N_2 atmosphere. Then 1 mmol% of DMAN, present in silica network, with respect to the methylene compound was added and the reaction started. Samples were taken periodically, and the evolution of the reaction was followed by GC and GC-MS equipped with an Equity-5 column (30 m*0.25*0.25 μm) and a FID as detector. For catalyst recycling studies, the solid was filtered and thoroughly washed with CH_2Cl_2 after each run and then outgassed at 373K for 12h to remove the adsorbed species. In all experiments, nitrobenzene was used as internal standard.

3. Results and Discussion

3.1 Synthesis and characterization of the hybrid materials

Organic-inorganic hybrids based on the disilylated-DMAN proton sponge inserted into the walls of non-ordered mesoporous silica have been synthesized following NH_4F-catalyzed sol-gel route at neutral pH and room temperature. These conditions allow binding covalently the functionalized DMAN fragments to the inorganic units, forming the framework of the mesoporous materials.

The presence of the organic moieties in the resultant solid was evidenced by means of elemental analysis. The C, H, N content and the calculated percentage in weight of organic species present into the solids are reported in Table 2.

Table 2. Organic content into the mesoporous hybrids estimated by elemental analysis (EA).

Samples	N%	C%	H%	Organic content (EA)/%
DMAN/SiO_2-0.1	0.07	0.7	0.8	1.57
DMAN/SiO_2-0.2	0.2	1.4	0.7	2.3
DMAN/SiO_2-0.5	0.3	1.8	0.8	2.9
DMAN/SiO_2-1	0.5	2.2	0.9	3.6
DMAN/SiO_2-5	2.2	8.5	1.9	12.6
DMAN/SiO_2-10	3.0	11.2	2.2	16.4
ADS-DMAN/SiO_2	3.4	18.0	2.9	24.3

The C/N/H ratio confirms that the organic corresponds to the proton sponge and no decomposition of the organic has occurred during the synthesis. However, it is observed that the experimental C/N ratio is higher that theoretical, this could be due the entrapment of some methanol molecules that occurs during the structuration of the hybrids. The presence of methanol has been evidenced by the ^{13}C MNR spectra of Fig.2. The organic content in the hybrids varies from 1.57% for the low loading to 16.4% for the highest loading DMAN/SiO_2 material, with a correlation between the amount of disilylated DMAN in the gel and the amount incorporated in the solid.

Thermogravimetric analysis was performed in order to gain insight, not only on the organic content presents in the solids, but also on the thermal stability of the inserted DMAN units with respect the pure DMAN or the simply adsorbed DMAN on SiO_2. Thus, the weight loss (TGA) and the DTA of the DMAN/SiO_2-5 hybrid, the adsorbed DMAN sample (ADS-DMAN/SiO_2) and pure DMAN molecule are reported in Figure 1. The first weight loss of the one-pot hybrid is observed at around 80-100°C and can be associated to the removal of physisorbed water. At higher temperature, the main weight loss is associated to the organic moieties (DMAN) and the organic content calculated between 150°C and 500°C, is similar to the results obtained by elemental analysis (see Tables 2 and 3). The DTA curves reveal that when DMAN is simply adsorbed on silica (ADS-DMAN/SiO_2, curve d), the decomposition of DMAN occurs at ca. 230°C, whilst the functionalized DMAN in the DMAN/SiO_2-5 hybrid (curve d) decomposes at higher temperature, close to 300°C. From these data, it can be concluded that the DMAN incorporated in SiO_2 framework (curve c) is more stable than DMAN adsorbed on SiO_2 (curve d) and much more stable than pure DMAN (curve e), that decomposes at ca. 150°C.

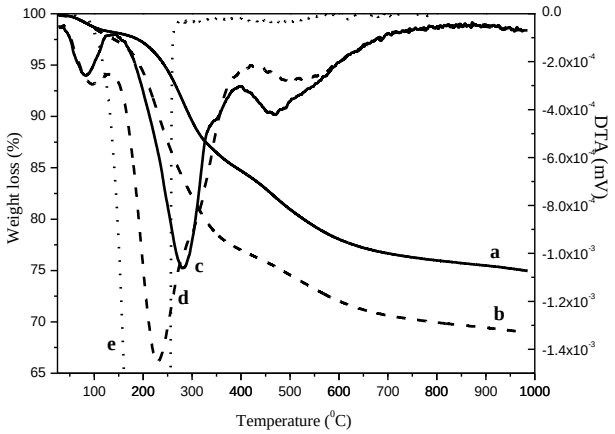

Fig.1 – TGA and DTA curves of DMAN/SiO_2-5 (curves a and c) and ADS-DMAN/SiO_2 (curves b and d). Curve e: DTA of pure DMAN.

Table 3.Weight loss (%) due to organic content calculated from TGA analysis.

Samples	wt% at 150°C	wt% at 500°C	Δwt% due to organic content	Organic content (EA)/%
DMAN/SiO_2-5	98.2	81.1	17.1	16.4
ADS-DMAN/SiO_2	97.5	74.6	22.9	24.3

To confirm that DMAN is chemically stabilized and covalently bounded into the silica framework of the one-pot hybrid materials, leaching tests were performed both on the DMAN/SiO_2 hybrids and on the sample prepared by adsorbing DMAN on SiO_2 (ADS-DMAN/SiO_2). For doing that, the as-synthesized materials were washed with ethanol at 298K for 3 days to remove the un-reacted DMAN species. In Table 4, the organic content of the as-synthesized samples and after the leaching tests of the hybrids and of the sample with physically adsorbed DMAN is reported.

The organic content (EA%), after the washing treatment in ethanol, clearly shows that in the case of physically adsorbed DMAN sample, the loss is ca. 9% (i.e. ~ 60% of the total amount of organic), whilst in the case of the DMAN/SiO_2 hybrids, the loss of organic content goes from 0.3% to 2% for the low and highly loaded materials. This result confirms that in the hybrids most of the functionalized DMAN is attached covalently to silica and not simply adsorbed. During the first day washing treatment, DMAN/SiO_2-5 hybrid loses most of the total loss, while during the second and the third days of washing only 0.3% and 0.1% of organic loss was observed respectively (Fig.S3). This is not the case for ADS-DMAN/SiO_2 sample that continuously leaches important amounts of organic (Fig.S3). The efficiency of the covalent DMAN incorporation in the silica matrix was evaluated from the N% content, measured by elemental analysis of the as-synthesized and washed hybrids (Table 4). The efficiency of organic incorporation decreases when increasing the DMAN loading. This means that a high loading in the synthesis gel does not ensure a higher level of organic incorporation into the silica network.

Table 4. Elemental analysis after the leaching tests and efficiency of DMAN incorporation into the SiO_2 network

Samples	As-synthesized hybrids				Washed hybrids					
	N/%	C/%	H/%	Organic content (EA)/%	N/%	C/%	H/%	Organic content (EA)/%	Organic loss/%	Efficiency of DMAN incorporation/%
DMAN/SiO_2-0.1	0.07	0.7	0.8	1.57	0.067	0.5	0.7	1.267	0.30	96
DMAN/SiO_2-0.2	0.20	1.4	0.7	2.30	0.19	1.2	0.6	1.99	0.31	95
DMAN/SiO_2-0.5	0.30	1.8	0.8	2.90	0.27	1.6	0.7	2.57	0.33	90
DMAN/SiO_2-1	0.50	2.2	0.9	3.60	0.44	1.7	0.7	2.84	0.76	88
DMAN/SiO_2-5	2.20	8.5	1.9	12.6	1.50	7.4	1.9	10.7	1.9	68
DMAN/SiO_2-10	3.00	11.2	2.2	16.4	2.00	10.3	2.1	14.4	2.0	66
ADS-DMAN/SiO_2	3.40	18.0	2.9	24.3	2.10	10.7	2.4	15.2	9.10	-

The results obtained up to now confirm that DMAN is intact into the hybrid materials and that most of the organic is not physically but it is probably covalently attached. However, at this point we need not only to reconfirm the integrity of the organic molecule in the final material, but specially the covalent insertion of the proton sponge into the network of the silica. To study this, we have made use of NMR spectroscopy. Specifically, the ^{13}C CP/MAS NMR spectra of the hybrids (Fig. 2, curves a and b) present the typical signals of DMAN (curve c) confirming the integrity of the organic moiety after the synthesis process. In the range between 150-110 ppm should appear the ^{13}C signals due to naphthalene groups,[25,26] while the peaks due to methyl groups belonging to $N(CH_3)_2$ should appear at 40-45 ppm. Indeed, the above signals are clearly seen in the ^{13}C spectra of the hybrid materials (curves a and b). However, in the hybrids, several other signals at 158.5, 61.3, 22.7 and 10 ppm also appear, that do not correspond to DMAN molecule. Then, the peak at 158.5 ppm is assigned to C=O groups and the other signals are due to C1 (10 ppm), C2 (22.7 ppm) C3 (61.3 ppm) of the $–CH_2$ groups belonging to the terminal silyl fragments of the functionalized DMAN (see the inset in Fig.2 for the labels of C atoms).[27]

The presence of these signals also confirm that the DMAN molecules were successfully functionalized. The different intensity of the ^{13}C signals in the hybrids spectra reflects the different DMAN loadings.

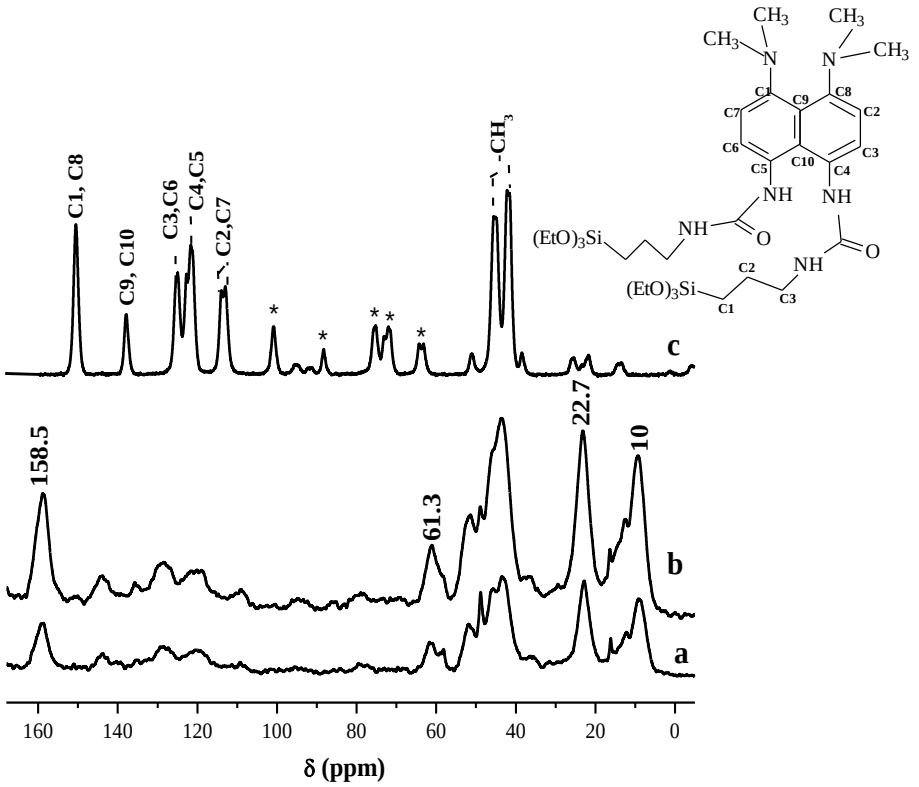

Fig. 2. ^{13}C-CP MAS NMR of DMAN/SiO_2-5 (curve a), DMAN/SiO_2-10 (curve b) and pure DMAN (curve c). * spinning bands.

^{29}Si MAS NMR spectra confirm that the DMAN fragments are not only intact after the synthesis of the hybrids but are also incorporated covalently into the non-ordered porous network bounded to inorganic silica units. In fact, the ^{29}Si MAS NMR spectra of the hybrids (Fig.3) exhibit bands from -50 ppm to -80 ppm assigned to T-type silicon species having a Si-C bond, being then confirmed that the hydrolysis and policondensation of silylated-DMAN occurs through alkoxy terminal groups of the silylated moieties. The intensity of the band corresponding to T-type silicon atoms is higher when the larger is the content of organic linkers into the hybrid frameworks. In addition, three peaks at -92, -100 and -110 ppm are also present, due to Q^2 ($Si(OH)_2(OSi)_2$), Q^3 ($Si(OH)(OSi)_3$) and Q^4 ($Si(OSi)_4$) silicon units respectively.[28] The incorporation of the disilylated DMAN into the framework of non-ordered mesoporous silica is also confirmed by the comparison of ^{29}Si NMR spectra of the hybrids with the pure disilylated DMAN (see inset of Fig.3). The DMAN-Si exhibits one peak centered at -45.7 ppm typical of Si-C bonds. When the DMAN-Si builders are finally inserted into the silica framework, the signal due to silicon atoms bounded to carbon units shifted in

the range -60 to -80 ppm, supporting the covalent incorporation of the disilylated organic species into the silica framework.

The integration of T and Q peaks in the ^{29}Si BD/MAS NMR spectra was performed to calculate the T/(Q+T) ratio and to evaluate the number of functionalized silicon atoms in the hybrids (Table 5). The Si_{func}/Si_{tot} ratio evidences that DMAN/SiO_2-10 has double Si atoms functionalized by organic linkers (~10%) than DMAN-SiO_2-5 (~5%), as expected considering the DMAN loading.

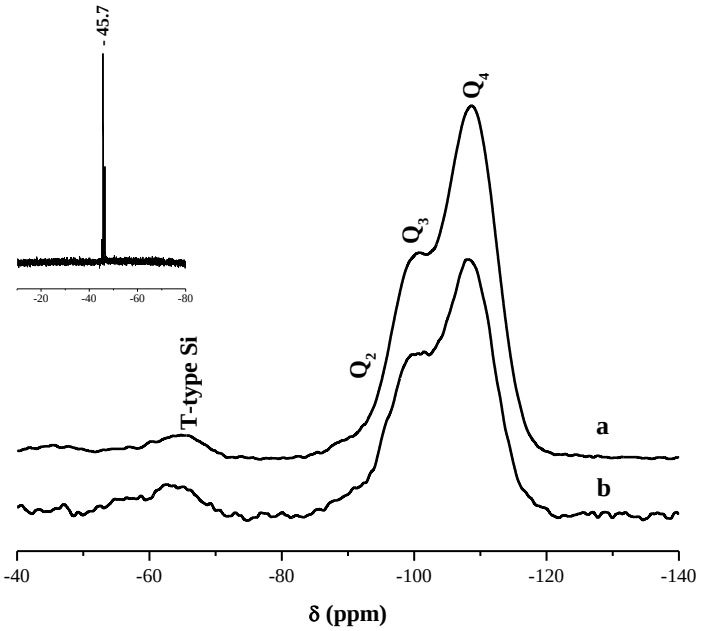

Fig. 3 ^{29}Si-BD MAS NMR of DMAN/SiO_2-5 (curve a) and DMAN/SiO_2-10 (curve b). In the inset, the ^{29}Si NMR spectrum of DMAN-Si is reported.

Table 5. Functionalized silicon atoms in the hybrids.

Samples	Si_{func}/Si_{tot} (NMR)
DMAN/SiO_2-5	0.048
DMAN/SiO_2-10	0.095

FTIR spectroscopy was used to investigate the surface vibration modes, confirming unambiguously the presence and integrity of organic DMAN builders in the network of the hybrid materials. In Fig. 4, the FTIR spectra of DMAN/SiO_2-10 (curve a) and DMAN/SiO_2-5 (curve b), outgassed at 100ºC to remove the adsorbed water, are reported. The spectrum of pure DMAN (curve c) is also reported for comparison. The spectra of the hybrids differ on the intensity of the bands due to the organic moieties. In the FTIR spectra of DMAN/SiO_2 hybrids outgassed at 100°C (curves a and b), the band at 2945 cm^{-1}, assigned to the C-H stretching mode of the $–CH_3$ in $N(CH_3)_2$ groups, and the band at 3045 cm^{-1} (weak), due to the -C-H stretching mode of the aromatic ring, can be observed.[29,30] The intense and broad absorption centered at 3370 cm^{-1} is due to the O-H stretching mode of Si-OH groups interacting with chemisorbed water or via H-bond. In the low frequency region, the bands at 1530 cm^{-1} and at lower wavenumber are associated to the stretching mode of the aromatic C=C, whilst the band at 1690 cm^{-1} is due to the stretching mode of the carbonyl group present in the functionalized DMAN. All these bands confirm the presence and the integrity of the functionalized DMAN into the hybrids.

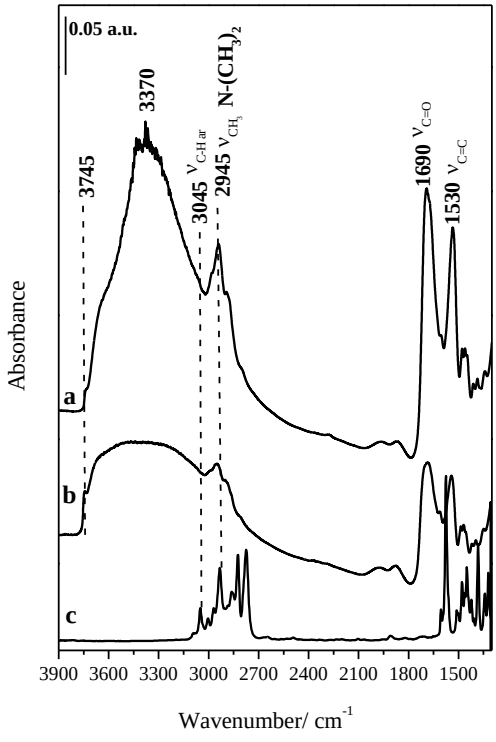

Fig. 4 FTIR spectra of DMAN/SiO_2-10 (curve a) and DMAN/SiO_2-5 (curve b) upon outgassing at 100°C. The spectrum of pure DMAN (curve c) is also reported.

In Fig. 5, the FTIR spectra of DMAN/SiO_2-5 upon thermal treatment are reported. When chemisorbed water is removed by outgassing at 200°C (curve b), a band at 3430 cm^{-1} is visible and

can be assigned to the stretching mode of N-H groups present in the functionalized DMAN fragments, in addition the band due to free silanols (3745 cm^{-1}) becomes evident. Upon outgassing at 400°C (curves c), the bands due to the organic moieties are still present but with lower intensity. In fact, at 400°C there is still a fraction of undecomposed organic units that have also been detected by DTA analysis (Fig.1).

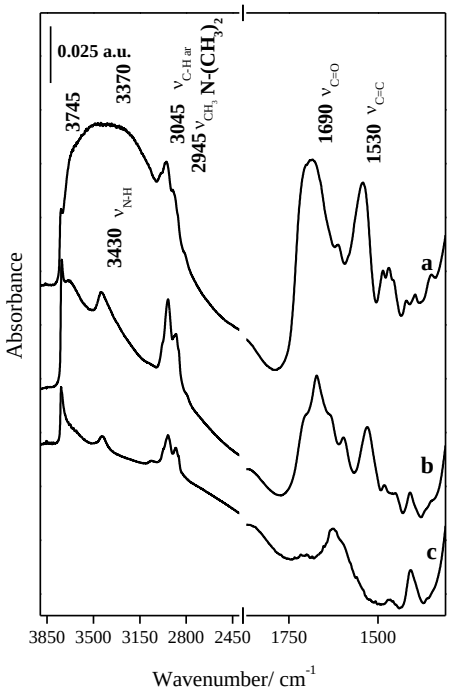

Fig.5 FTIR spectra of DMAN/SiO_2-5 upon outgassing at 100°C (curve a), 200°C (curve b) and 400°C (curve c).

3.2 Textural properties of the hybrid materials

The textural properties measured by N_2 adsorption are reported in Table 6 and compared to a pure SiO_2 and to DMAN adsorbed on SiO_2 (ADS-DMAN/SiO_2) sample.

Table 6. Textural properties of the DMAN/SiO_2 hybrids.

Samples	SSA_{BET} $SSA(m^2/g)$	External SA (m^2/g)	Pore size Å	Pore volume cm^3/g
Pure SiO_2	797	791	27	0.3
DMAN/SiO_2-0.1	763	752	28	0.3
DMAN/SiO_2-0.2	752	750	28	0.28
DMAN/SiO_2-0.5	725	718	27	0.28
DMAN/SiO_2-1	600	592	26	0.23

DMAN/SiO_2-5	455	450	30	0.24
DMAN/SiO_2-10	329	320	30	0.17
ADS-DMAN/SiO_2	150	150	49	0.15

The BET specific surface area (SSA) of the hybrids varies from 763 to 329 $m^2\ g^{-1}$ depending on the DMAN loading. A marked decrease in the SSA can be observed when the structural organic content is higher, probably due to the more difficult structuration of DMAN fragments into the porous framework. However, in all cases, the SSAs and pore volumes obtained are in the mesoporous range, being practically negligible the microporous contribution (Table 6). This can also be deduced from the shape of the adsorption isotherms (Fig. 6A) that are typical of non-ordered mesoporous systems. In particular, all the hybrids show an isotherm with the inflexion point between 0.6-0.8 p/p_0 while the inflexion point of the silica with adsorbed DMAN (ADS-DMAN/SiO_2) is present at high value of p/p_0, meaning that the pore diameter is larger than for the other hybrids. The pore distribution of the DMAN/SiO_2 samples (see Fig.6B) are narrow and the mean pore diameters are centered at 30 Å, while the ADS-DMAN/SiO_2 sample shows a broader distribution. The physically adsorbed DMAN on silica has a low SSA and pore volume compared to the other hybrids and shows a broad distribution in the pore sizes, due probably to inhomogeneous distribution and a partial blockage of porous by the adsorbed DMAN.

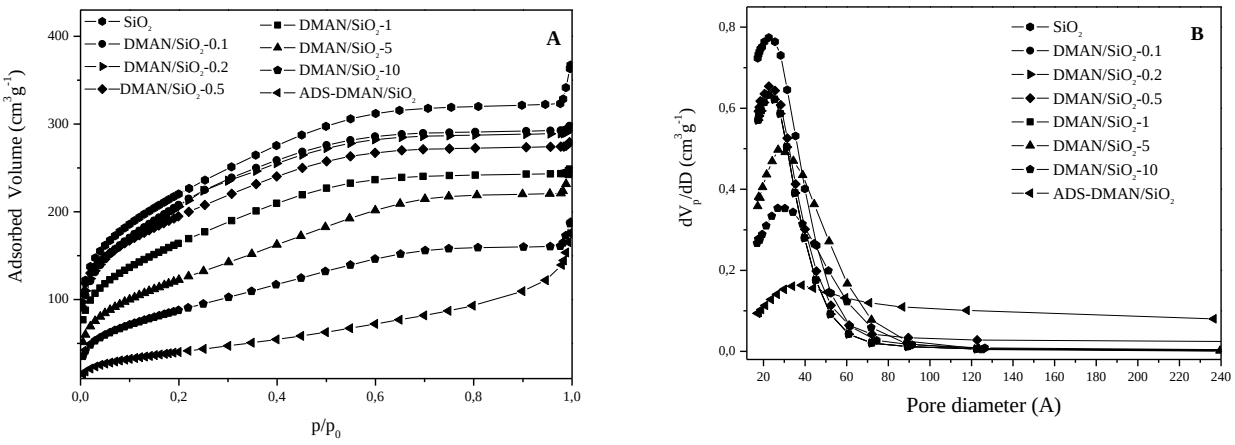

Fig. 6 Section A: N_2 adsorption isotherms and Section B: Pore size distribution, calculated by BJH method, of DMAN/SiO_2 hybrids with different DMAN loading, ADS-DMAN/SiO_2 and pure SiO_2.

All samples show an increase of the specific surface area upon the washing treatment with ethanol (Table 7). This observation indicates that after the one-pot synthesis there are some DMAN

molecules that are simply adsorbed inside the mesopores, partially blocking the channels. The adsorbed molecules are removed after washing and consequently the specific surface area increases. In this way, during the first day of washing, the SSA of DMAN/SiO_2-5 hybrid material increases from 455 to 540 m^2g^{-1} and during the second and the third days only a slight increase of the SSA is observed (see Fig. S4). This tendency is also observed with all hybrid materials here synthesized.

Table 7. Textural properties of the DMAN/SiO_2 hybrids after the leaching tests

Samples	SSA_{BET} (m^2/g)	External SA (m^2/g)	Pore size Å	Pore volume cm^3/g
DMAN/SiO_2-5 as-synthesized	455	450	30	0.24
washed	569	560	30	0.26
DMAN/SiO_2-10 as-synthesized	329	320	30	0.17
washed	453	450	30	0.21
ADS-DMAN/SiO_2 as-synthesized	150	150	49	0.15
washed	268	269	49	0.19

3.3 Catalytic tests

The basicity of the hybrid materials, containing proton sponges as catalytic organic builders, was tested for the Knoevenagel reaction of benzaldehyde (1) and ethyl cyanoacetate (2) (pK_a = 9) with ethanol at 333K (Scheme 3). The use of ethanol as solvent is due to a previously work,[21] that showed that a polar protic solvent was the most effective for the formation of the trans-α-ethyl-cyanocinnamate (product 3).

The Knoevenagel condensation of carbonyl compounds is widely used in organic synthesis to produce important intermediates and end products for perfumes, pharmaceutical and polymers.[31,32] The reaction can be catalyzed by strong and weak basicities depending on the level of activation of the reactant containing methylenic activated groups, being therefore an adequate reaction for comparing catalysts with different basicities. The kinetics of the Knoevenagel reaction is generally considered to be a first order reaction with respect to each reactant and the catalysts.[19,33-35]

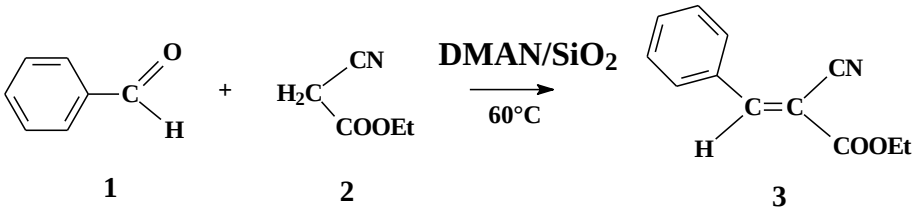

1 2 3

Scheme 3 – Scheme of the Knoevenagel reaction of benzaldehyde and ethyl cyanoacetate.

In Fig. 7, the yields for product (3) obtained with the DMAN/SiO_2 hybrids are reported. The DMAN/SiO_2-0.5 and DMAN/SiO_2-0.2 hybrids show better catalytic performances than the hybrids with higher DMAN loadings. In fact, 100% conversion is achieved after 6h of reaction, with 100% of selectivity. Using DMAN/SiO_2-1, 98% yield was produced; whilst using DMAN/SiO_2-5 and DMAN/SiO_2-10, 93% and 78% conversion was respectively obtained at the same reaction time. This behavior suggests that a high concentration of basic sites has a detrimental effect on the catalytic activity. In fact, well isolated and separated basic sites are usually needed to have a good base catalyst.[36] The activity of the very low loading hybrid (DMAN/SiO_2-0.1) lies between DMAN/SiO_2-5 and DMAN/SiO_2-10, meaning that, in this sample, the concentration of the basic sites is too low to perform a high catalytic activity. In addition, DMAN/SiO_2-0.5 shows a higher yield at low reaction time and reaches the yield of homogenous DMAN after 4h reaction. The Turnover frequencies calculated after 1h reaction, reported in Table 8, follow the trend observed in Fig.7, in fact the DMAN/SiO_2-0.5 hybrid shows the highest TOF that is close to the one of the homogeneous DMAN.

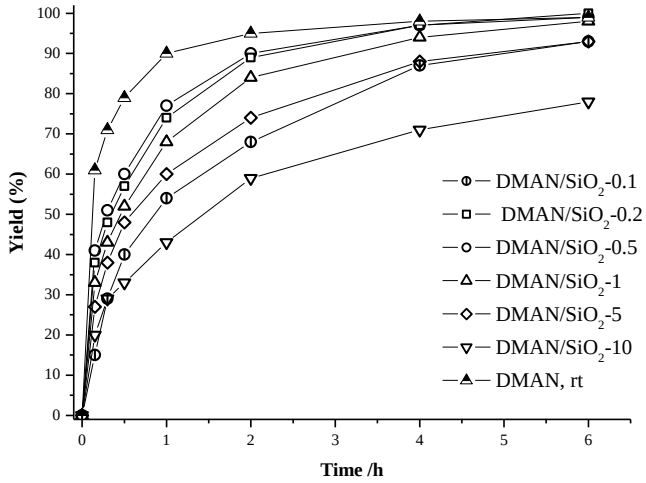

Fig. 7 - Knoevenagel condensation of benzaldeyde with ethyl cyanoacetate using heterogeneous hybrid catalysts at 333K with ethanol. The yield of homogeneous DMAN at room temperature is also reported for comparison.

Table 8. Initial kinetic constant calculated at 10 min and Turnover frequencies (TOF) calculated at 1h.

Catalysts	Yield (%)		Inicial kinetic constant/min	TOF/min
	2h	6h		
DMAN/SiO_2-0.1	54	93	0.7	90
DMAN/SiO_2-0.2	74	100	3.8	123
DMAN/SiO_2-0.5	77	100	4.1	128
DMAN/SiO_2-1	68	98	3.3	113
DMAN/SiO_2-5	60	93	2.7	100
DMAN/SiO_2-10	43	78	2	72
Pure DMAN	90	100	6.1	150

Catalyst deactivation and reusability was studied with DMAN/SiO_2-0.5. The yields after recycling the catalyst are reported in Fig. 8 after 2h and 6h of reaction. The yields calculated after 2h evidence that there is a slightly decrease after each catalytic runs, whilst after 6h, the yields are almost similar for the first three catalytic runs and then decreased. The elemental analysis performed on the used catalyst, after washing with CH_2Cl_2, reveals that no leaching has occurred from 1 to 3 runs whilst after the third run 0.2% of leaching, due to DMAN loss, has occurred explaining the decrease in the observed yield. The leaching observed after the third run, could be due to the temperature and solvent effect.

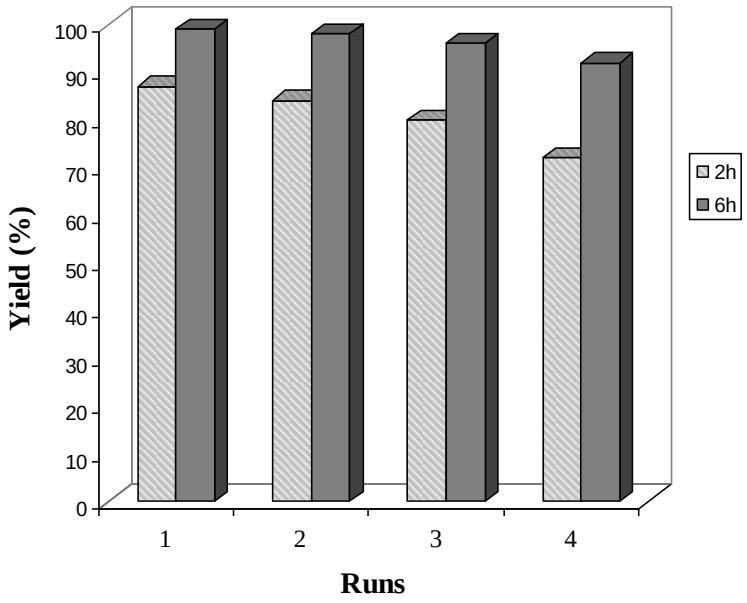

Fig. 8 – Recycling tests of Knoevenagel condensation of using DMAN/SiO_2-0.5 with ethanol at 333K. The yield (%) is reported after 2h and 6h of reaction.

From the results obtained, it appears that the mesoporous hybrid materials, synthesized in absence of SDA by means of a simple procedure and containing proton sponges as organic building block, offer possibilities for base catalysis. Moreover, the method of synthesis open the possibility of combining these basic sites with other acid and/or redox and to generate multisite catalysts for carrying out cascade type or one-pot multistep reactions.

Conclusions

By working at room temperature and pH=7 with NH_4F catalyzed sol-gel synthesis, non ordered organic-inorganic mesoporous hybrids have been obtained by the insertion of proton sponges fragments bonded to silica units. The study performed has shown the effective integration of organic builders into the mesoporous framework preserving the basic properties of the proton sponges. The absence of SDAs and the use of soft synthesis conditions are validated in the study here presented, being possible to design functional hybrid materials which contain stable, isolated and active basic sites able to carry out condensation processes to form carbon-carbon bonds. In addition, the loading of proton sponge inside the silica framework strongly influences the catalytic performances. These hybrids are the first step for the designing multifunctional catalysts by the insertion of acid-base and acid- redox functions within the mesoporous structure.

Acknowledgments

The authors thank financial support by Consolider-Ingenio (MULTICAT project) from Spanish Government. EG thanks Marie Curie Fellowship (FP7-PEOPLE-2009-IEF**)** for financial support.

References

1 F. Hoffmann, M. Cornelius, J. Morell, M. Fröba, *Angew. Chem. Int. Ed*., 2006, **45**, 3216-3251.

2 C. Sanchez, L. Rozes, F. Ribot, C. Laberty-Robert, D. Grosso, C. Sassoye, C. Boissiere, L. Nicole, *C.R. Chimie*, 2010,**13**, 3-39.

3 C. Sanchez, B. Juliàn, P. Belleville, M. Popall, *J. Mater. Chem*., 2005, **15**, 3559-3592.

4 A.P. Wight, M.E. Davis, *Chem Rev*., 2002, **102**, 3589-3614.

5 K. Vallé, P. Belleville, F. Pereira, C. Sanchez, *Nat. Mater*., 2006, **5**, 107-111.

6 M.P. Kapoor, S. Inagaki, *Bull. Chem. Soc. Jpn*., 2006, **79**, 1463-1475.

7 U. Damrau, H.C. Marsmann, *J. Non-Cryst. Solids*, 1994, **168**, 42-48.

8 N.K. Raman, T.L. Ward, C.J. Brinker, R. Sehgal, D. M. Smith, Z. Duan, M. Hampden-Smith, *Appl. Catal. A: General*, 1993, **69**, 65-82.

9 B. Boury, R.J.P. Corriu, *Chem.Commun*., 2002, 795-802.

10 A. Mehdi, C. Reye, R.J.P. Corriu, *Chem.Soc.Rev*., 2011, **40**, 563-574.

11 E.J.A. Pope, J.D. Mackenzie, *J. Non-Cryst. Solids*, 1986, **87**, 185-198.

12 R. Winter, J.B. Chan, R. Frattini, J. Jonas, *J. Non-Cryst. Solids*, 1988, **105**, 214-222.

13 E. Reale, A. Leyva, A. Corma, C. Martinez, H. Garcia, F. Rey, *J. Mater. Chem*., 2005, **15**, 1742-1754.

14 U. Diaz, T. Garcia, A. Velty, A. Corma, *J. Mater. Chem*., 2009, **19**, 5970-5979.

15 R.W. Alder, P.S. Bowman, W.R. Steele, D.R.Winterman, *J. Chem. Soc., Chem. Commun*., 1968, 723-724.

16 R.W. Alder, *Chem. Rev*., 1989, **89**, 1215-1223.

17 A.L. Llama-Saiz, C. Foces-Foces, J. Elguero, *J. Mol. Struct*., 1994, **328**, 297-323.

18 S.T. Howard, *J. Am. Chem. Soc*., 2000, **122**, 8238-8244

19 I.Rodriguez, G. Sastre, A. Corma, S. Iborra, *J. Catal*., 1999, **183**, 14-23.

20 M.J. Climent, A. Corma, I. Dominguez, S. Iborra, M.J. Sabater, G. Sastre, *J. Catal*., 2007, **246**, 136-146.

21 A. Corma, S. Iborra, I. Rodriguez, F. Sanchez, *J. Catal*., 2002, **211**, 208-215.

22 S. J. Gregg, K. S. W. Sing, Adsorption, Surface Area and Porosity, Academic Press, London, 1982.

23 K. S. W. Sing, D. H. Everett, R. A. W. Haul, L. Moscou, R. A. Pierotti, J. Rouquerol, T. Siemieniewska, *Pure Appl. Chem*., 1985, **57**, 603-619.

24 E. P. Barrett, L. G. Joyner and P. P. Halenda, *J. Am. Chem. Soc*., 1951, **73**, 373-380.

25 K. Woźniak, *J. Mol. Struct*., 1996, **374**, 317-326.

26 A.F. Pozharskii, *Russian Chem. Rev.*, 1998, **67**, 1-24.

27 Y. Seo, S. Park, D.H. Park, *J. Solid State Chem*., 2006, **179**, 1285-1288.

28 K. Kawahara, Y. Hagiwara, A. Shimojima and K. Kuroda, *J. Mater. Chem*., 2008, **18**, 3193-3195.

29 L. van Meervelt, K. Platteborze, Th. Zeegers-Huykens, *J. Chem. Soc. Perkin Trans*., 1994, **2**, 1087-1090.

30 B. Brzeziński, G. Schroeder, E. Grech, Z. Malarski, L. Sobczyk, *J. Molec. Structure*, 1992, **274**, 75-82.

31 I. Rodriguez, S. Iborra, F. Rey, A. Corma, *Appl. Catal. A: General*, 2000, **194-195**, 241-252.

32 M.J. Climent, A. Corma, S. Iborra, K. Epping, A. Velty, *J. Catal*., 2004, **225**, 316-326.

33 F.S. Prout, U.D. Beaucaire, G.R. Dyrkarcz, W.M.Koppes, R.E. Kuznicki, T.A. Marlewski, J.A. Pienkowski, J.M. Puda, *J. Org. Chem*., 1973, **38**, 1512-1517

34 G. Jones, *Org. React*., 1967, **15**, 204-599.

35 J. Guyot, A. Kergomard, *Tetrahedron*, 1983, **39**, 1161-1166.

36 K. Motokura, S. Tanaka, M. Tada, Y. Iwasawa, *Chem. Eur. J*., 2009, **15**, 10871-10879.